PAPER

Check for updates

Characterization of the oxygen properties of a hybrid glass chip designed for precise on chip oxygen control†

Charlotte Bouquerel, [iD] [abc] Simon Dumas,[a] Elias Abedelnour,[de] Ester Simkova, [iD] [a] Giacomo Gropplero,[a] Linda Meddahi,[a] Bertrand Cinquin,[f] Michael Tatoulian, [iD] [d] William César[c] and Stephanie Descroix [iD] *[a]

Despite its relevance in several research fields, the regulation of dissolved gas concentration in microfluidic chips remains overlooked. Precise control of dissolved oxygen levels is of importance for life science applications, especially for faithfully replicating *in vivo* tissue conditions in organ-on-chips. The current methods to control oxygen on-chip rely on the use of chemical scavengers, on the integration of an additional gas channel or on the perfusion of a liquid pre-equilibrated at a set oxygen level. However, for precise oxygen control, these microfluidic devices must be made from gas-impermeable materials. In this regard, glass is a material of choice due to its complete impermeability, but its microfabrication often requires specific clean room processes. Here, we report a low-tech fabrication method for a hybrid glass chip, which involves assembling glass components using an adhesion process. To evaluate this chip's suitability for use under highly controlled oxygen conditions, we developed a two-step assessment protocol. This involved determining the time needed to reach a target oxygen level during perfusion and measuring the reoxygenation time following the cessation of flow. Based on a dual approach of simulations and experiments, we emphasized crucial adhesive properties such as oxygen diffusion and solubility and proposed a range of well-suited adhesive materials. Finally, we demonstrated the interest of this hybrid glass chip for on-chip cell culture and cell respiration measurements. This work paves the way for broader accessibility in producing low tech gas-tight microfluidic chips for diverse applications.

Introduction

Control of the oxygen level is critical for biological applications such as *in vitro* cell culture models. In the human body, the oxygen level is known to drastically vary among organs with an oxygen range between 1 and 18.9%.[1] For instance, lung alveoli experience approximately an oxygen partial pressure (pO$_2$) of 144 mmHg (18.9%), whereas 43 mmHg (5.6%) can be measured in peri-bronchial lung tissues,

[a] *Macromolécules et Microsystèmes en Biologie et Médecine, UMR 168, Institut Curie, Institut Pierre Gilles de Gennes, 6 rue Jean Calvin, 75005, Paris, France. E-mail: stephanie.descroix@curie.fr*

[b] *Stress et Cancer, Inserm, U830, Institut Curie, Equipe labelisée par la Ligue Nationale Contre le Cancer, PSL Research University, 26 rue d'Ulm, 75005, Paris, France*

[c] *Fluigent, 67 avenue de Fontainebleau, 94270, Le Kremlin-Bicêtre, France*

[d] *Chimie ParisTech, PSL University Paris, CNRS, Institut de Recherche de Chimie Paris, UMR8247, 11 rue Pierre et Marie Curie, 75005 Paris, France*

[e] *Sanofi, Integrated Drug Discovery – IDD France, 1 Avenue Pierre Brossolette, Chilly Mazarin, France*

[f] *UMS 3750, Institut Pierre Gilles de Gennes, 6 rue Jean Calvin, 75005, Paris, France*

† Electronic supplementary information (ESI) available. See DOI: https://doi.org/10.1039/d4lc01017e

65 mmHg (8.5%) in the breast, 26 mmHg (3.4%) in the brain, and 8 mmHg (1%) in the skin epidermis.[2] These values can be even further modified under pathological conditions.

The current main method for on-chip oxygen control involves integrating a gas channel separated from the liquid channel by a membrane. These membrane-based liquid degassing systems are also commonly employed in conventional chemistry.[3,4] Using this method, Koens *et al.*[5] were able to reach on-chip 0.3% oxygen in 15 min. In another approach, gas and liquid streams can also flow together without a membrane by introducing a fast-flowing gas stream together with a slow liquid flow.[6] However, the gas consumption rate is very high and can lead to liquid evaporation. Chemical scavengers such as pyrogallol or Na$_2$-SO$_3$[7] can also be used to control the on-chip oxygen level. However, scavenging reagents are shown to potentially interfere with cell culture conditions. An alternative method consists of perfusing the chip with a pre-equilibrated liquid at a set oxygen level.[8,9] This method is compatible with any chip design and has a lower gas consumption rate.

Importantly, to finely control on-chip oxygen levels, microfluidic chips must be made of gas-tight materials.

This prevents oxygen diffusion from ambient air through chip walls leading to an uncontrolled oxygen level. However, there is currently a limited understanding of the oxygen-related properties of materials commonly used in microfluidic chips. Among the materials readily available for microfabrication, cyclic olefin copolymer (COC) and polymethyl methacrylate (PMMA) offer the lowest oxygen diffusion coefficient (10^{-12} m^2 s^{-1}, 1000 times lower than PDMS (10^{-9} m^2 s^{-1})).[10] However, previous work has shown that low pO_2 levels (such as 15 mmHg) cannot be reached in a COC channel while perfusing the chip with a 15 mmHg pre-equilibrated liquid at a moderate flow rate (<10 μL min^{-1}). Thanks to its gas impermeability, glass emerges as a material of choice for on-chip oxygen control.[9] Other interesting properties of glass include high electrical resistivity, low thermal conductivity, broad light transmittance, and resistance to organic solvents. However, fabrication processes of glass-based devices often require specific clean-room facilities,[11] and the resulting microfluidic chips are usually expensive. For example, clean room facilities are often needed to seal microfluidic chips by anodic bonding or fusion bonding of glass components. Recent work highlighted clean-room free processes assembling glass components with adhesive layers such as a thin silicon layer,[12] water as a bonding agent[13] or even double-sided tape.[14] However, the effect of these adhesive layers on the oxygen permeability of the hybrid glass chip has been overlooked. A low-tech, easy-to-handle solution with highly controlled materials for on-chip oxygen control still needs to be developed along with a methodological approach for scrutinizing the impact of the chip material on oxygen control.

Inspired by the simplicity of this assembling approach, we proposed a simple and low-cost fabrication process for a hybrid glass–adhesive chip and investigated how the properties of the adhesive layer influence on-chip oxygen control. The ability of the hybrid device to operate under oxygen-controlled conditions is quantitatively assessed through a two-step protocol: (i) first, perfusing the chip with pre-equilibrated water set at a precise low oxygen level to measure the time required to reach the target, and then (ii) measuring the reoxygenation rate after cessation of the flow. Using material properties similar to those of common chip materials (PDMS and COC), finite element simulations disentangled the effects of oxygen diffusion, solubility and geometrical parameters of the adhesive on the oxygen control of the hybrid chip. Strikingly, the results showed that even though the adhesive's surface area within the fluidic channel represents only 5% of the whole surface, both adhesive properties and geometrical features can significantly impede on-chip oxygen control. We then identified epoxy adhesive as a promising candidate for developing a hermetic low-tech hybrid glass–epoxy chip, due to its very low solubility and diffusivity to oxygen. Finally, the potential of this hybrid glass–epoxy chip is demonstrated for cell biology applications by quantitatively measuring cell respiration in an oxygen-controlled environment.

Results

Experimental protocol for characterizing the hybrid chip oxygen permeability properties

Given that COC is often considered as a gas-impermeable material, we first performed finite element simulations to assess the potential of on-chip oxygen control in a full COC chip. COMSOL simulations showed that for a COC channel (3 mm × 37 mm × 1 mm) perfused at 10 μL min^{-1} with a liquid at a pO_2 of 15 mmHg, the pO_2 inside the chip stabilizes at around 30 mmHg after a few minutes (Fig. S1†). A pO_2 of 15 mmHg cannot be reached on-chip within 2 hours of perfusion. This limited pO_2 can be attributed to the continuous entry of oxygen diffusing from COC walls into the channel. Additionally, notable reoxygenation occurred after flow cessation, with an increase of +41 mmHg within 2 h. Similar experiments previously performed by our group confirmed these simulations.[9] These combined experiments and simulations highlighted that precise oxygen control at a low flow rate or under static conditions cannot be achieved in COC chips.

Glass offers a promising alternative to COC due to its gas-impermeable properties. However, glass chip fabrication often necessitates specific clean-room facilities, particularly for glass chip bonding. Building on the glass–adhesive assembly methods already widely adopted by the community, we explored whether this assembly method could be used in the context of on-chip oxygen control. Specifically, we examined how a thin adhesive layer used to assemble glass components affects the oxygen permeability of the glass chip. To produce the hybrid glass–adhesive chip, we followed a straightforward protocol that involved assembling three glass slides with two adhesive layers (Fig. 1A). The glass slides were perforated by laser ablation to create the inlet/outlet and the channel chamber. Before the assembly, an oxygen sensor was positioned at the bottom of the chip to enable continuous monitoring of the on-chip oxygen level (see the Experimental section). The oxygen level in the glass–adhesive chip depends on the contribution of three phenomena: oxygen diffusion between ambient air and the adhesive edges, oxygen diffusion between the adhesive center and the fluidic channel, and the advection in the fluidic channel (Fig. 1B).

To select the optimal adhesive material, we developed a two-step characterization protocol (Fig. 2). In a first step, a liquid pre-equilibrated at an oxygen partial pressure of 15 mmHg (which corresponds to the oxygen level in lung tumors[15]) is flowed into the microfluidic channel. This channel initially contains air under ambient conditions, with a pO_2 of 159 mmHg. The time required to decrease the pO_2 from 159 mmHg to 15 mmHg (±10%) for a liquid flow rate of 10 μL min^{-1} is then measured. A second step is performed to study the stability of maintaining this oxygen level over time: after 1 h of liquid perfusion at low pO_2, the flow is stopped and the amplitude of the on-chip reoxygenation (ΔpO_2) is measured over 2 h.

To evaluate the impact of the adhesive layer, different properties were evaluated. The first one is the adhesive
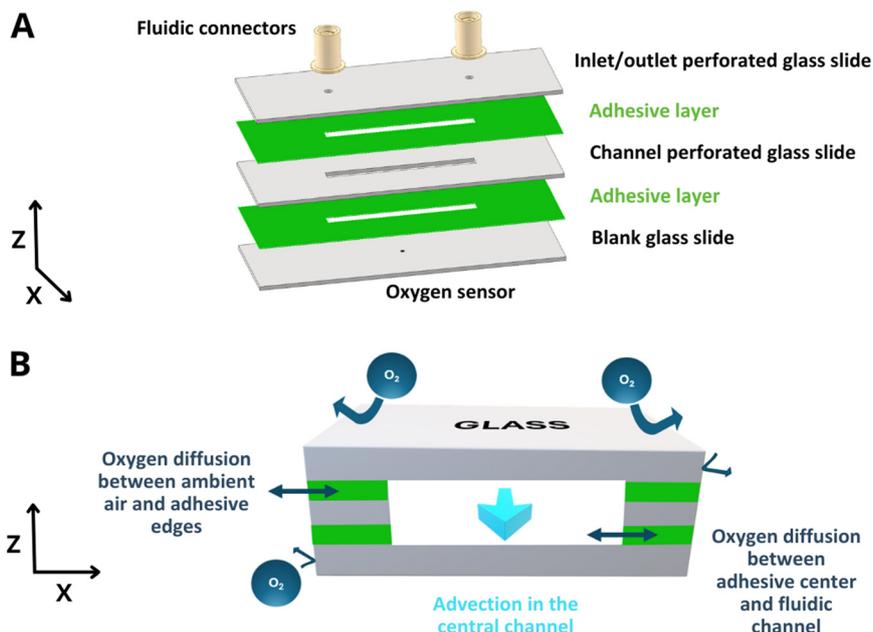
Fig. 1 (A) Schematic representation of a five-layer chip assembly: glass slides are in grey, and adhesive layers are in green. (B) The oxygen control properties in the adhesive–glass chip depend on the combination of three phenomena: the oxygen diffusion between ambient air and the adhesive edges, the oxygen diffusion between the adhesive center and the fluidic channel, and the advection in the fluidic channel of a liquid pre-equilibrated at a set oxygen level. Dark blue arrows indicate the direction of oxygen transfer.
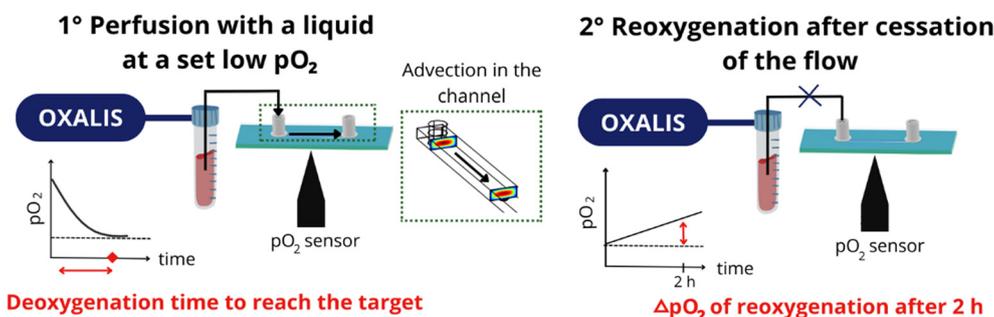

Fig. 2 Characterization protocol of the microfluidic chip oxygen permeability properties. First, the chip was perfused with a liquid pre-equilibrated at a set low pO_2 (15 mmHg) and we measured the deoxygenation time to reach the target. In a second step, the flow was stopped, and we measured the on-chip reoxygenation. Oxygen levels were controlled in the inlet reservoir using an Oxalis system.[9]

geometry that sets the total volume of adhesive as well as the surface of contact adhesive/liquid and adhesive/ambient air. On-chip oxygen control also depends on the adhesive intrinsic properties, as they influence oxygen diffusion through the chip material. The final parameter to consider is the advection within the fluidic channel that carries the pre-equilibrated liquid. At very high flow rates (*e.g.* 100 μL min^{-1}), the choice of adhesive material becomes less significant, as the advective transport rate surpasses the diffusive transport rate. At lower flow rates, the selection of low oxygen diffusive adhesive may become crucial. To be compatible with a wide range of applications, including biological studies where low shear stress is required, the hybrid glass chip should allow precise oxygen control while minimizing the flow rate. Under these conditions, the adhesive's intrinsic properties

particularly the oxygen diffusion coefficient and solubility must be carefully examined.

The diffusion of oxygen in the adhesive material can be described by Fick's law: $J = -D\nabla[O_2]_{adhesive}$ with J (mol s^{-1} m^{-2}) being the diffusion flux, D (m^2 s^{-1}) the diffusion coefficient, and $\nabla[O_2]_{adhesive}$ (mol m^{-4}) the oxygen concentration gradient in the adhesive between ambient air pO_2 = 159 mmHg (20.9% at P_{atm} = 760 mmHg) and deoxygenated perfused liquid pO_2 = 15 mmHg. The diffusion coefficient depends on the material properties, for example in the case of a polymeric material, it depends on the degree of cross-linking, the presence of pinholes, the molecular organization, and the degree of crystallinity.[16]

The material solubility quantifies the oxygen saturation in the material at equilibrium and is described by Henry's law: $S = [O_2]_{eq} = K_h pO_{2(air)}$, where $[O_2]_{adhesive\_eq}$ (mol m^{-3}) is the

oxygen concentration at equilibrium in the material, also called solubility (S), pO_2 (mmHg) is the oxygen partial pressure in air and K_h (mol m^{-3} mmHg^{-1}) is the Henry's coefficient of the air/material interface. Oxygen solubility depends on both the material chemistry and its affinity for oxygen.[16] Similarly, the solubility ratio of oxygen between the liquid and the material is described by a partition coefficient K_p with $K_p = \dfrac{[O_2]_{water\_eq}}{[O_2]_{adhesive\_eq}}$. Most adhesive materials exhibit a non-negligible oxygen solubility. Even COC renowned for its low gas permeability presents a rather high oxygen solubility (S = 1.12 mol m^{-3}).

Influence of the adhesive oxygen solubility and oxygen diffusion rate on the oxygen control properties of the hybrid glass chip

To evaluate the impact of adhesive properties, specifically oxygen diffusion and solubility, on oxygen control, we first performed a finite element analysis using COMSOL. The analysis was performed with a 5-layer chip (3 layers of glass and 2 layers of adhesive) modelized in 3D as described in the Experimental section, Table S1, and Fig. S2.† The adhesive layer did not cover the top and bottom of the fluidic channel (Fig. 1). Using these simulations, we examined the variation of on-chip oxygen levels over time during the perfusion at 10 μL min^{-1} of a liquid with a pO_2 of 15 mmHg. Additional simulations were performed for higher flow rates (40 and 100 μL min^{-1}) (Fig. S3†).

To model the impact of the adhesive oxygen solubility and diffusion coefficient on the on-chip oxygen control, the simulations were first performed with two adhesive materials experimentally compatible with glass bonding and commonly used in microfabrication: COC and PDMS. PDMS is highly oxygen permeable (D = 3.4 × 10^{-9} m^2 s^{-1}, S = 1.69 mol m^{-3}), while COC is supposed to be moderately oxygen permeable (D = 4.6 × 10^{-12} m^2 s^{-1}, S = 1.12 mol m^{-3}). As expected, our simulations evidenced that PDMS adhesive layers cannot be used for the hybrid glass chip as the target oxygen partial pressure is unreachable when perfusing the chip for 30 min with pO_2 plateauing at 50 mmHg (Fig. S4†). This lack of oxygen control can be attributed to the rapid diffusion of oxygen within the PDMS adhesive layer, leading to the formation of a broader gradient compared to adhesive materials with lower diffusivity. In contrast, for a glass–hybrid chip assembled with a 100 μm adhesive layer made of COC, the target pO_2 is reached within 30 min (Fig. S4†).

To independently assess the effect of oxygen diffusion and solubility, a broad range of oxygen diffusion coefficients from 10^{-12} to 10^{-8} m^2 s^{-1} was studied for a constant solubility of S = 1.12 mol m^{-3}. Then, in a second step, a range of solubility coefficients from 0.5 to 3 mol m^{-3} was tested for a constant diffusion coefficient of D = 4.6 × 10^{-12} m^2 s^{-1}. Compared to the diffusion coefficient range, the range of oxygen solubility investigated is narrower as the oxygen solubility between materials of low permeability (COC) and high permeability

(PDMS) is known to be limited.[17] All these conditions were tested with adhesive layers of 100 μm thickness and fully covering the width and length of the glass slides except the channel bottom and top.

For all conditions, the simulations showed a decrease in dissolved oxygen from ambient conditions to a plateau throughout the perfusion of deoxygenated water in the channel (Fig. 3). The plateau value ideally should be 15 mmHg, corresponding to the set oxygen level of the perfusing liquid. However, it may be significantly higher depending on the oxygen diffusion characteristics of the adhesive. Due to the asymptotic convergence of the curve, which theoretically approaches the target without actually reaching it, it was decided to define the time of perfusion as the time taken to reach ±10% of the target 15 mmHg. As shown in Fig. 3A, the slope of the deoxygenation curve does not significantly vary with the oxygen diffusion coefficient of the adhesive material (−26.5 mmHg min^{-1} for D = 10^{-12} m^2 s^{-1} and −29.8 mmHg min^{-1} for D = 10^{-8} m^2 s^{-1}, see Table S2†). In contrast, the value of the final pO_2 plateau strongly varied with the oxygen diffusion rate. This final pO_2 value is around 15 mmHg for D = 10^{-12} m^2 s^{-1} and 35 mmHg for D = 10^{-8} m^2 s^{-1}. The oxygen diffusion rate also impacts the time required to reach the target level of oxygen when feasible. For an adhesive material of D = 10^{-12} m^2 s^{-1}, the target pO_2 is achieved in 25 min, whereas for D higher than 10^{-11} m^2 s^{-1}, the target is not reached after 60 min. We next studied the effect of D on the reoxygenation after flow cessation (ΔpO_2/2 h). We observed in the glass–adhesive chip a reoxygenation of 112 mmHg for an adhesive material of D = 10^{-8} m^2 s^{-1}, whereas it was only 3.5 mmHg for an adhesive material of D = 10^{-12} m^2 s^{-1} (Fig. 3B). Overall, these simulations showed that adhesive materials with a diffusion coefficient equal to or lower than 10^{-12} m^2 s^{-1} give optimal performances: a time to reach the target of 25 min and reoxygenation limited to 3.5 mmHg.

We next tested the impact of the material oxygen solubility and evidenced that adhesives with higher solubility increase the time to reach the target inside the channel: a pO_2 of 15 mmHg (±10%) is reached in 22 and 43 min using chips assembled with adhesives of S = 0.5 and 3 mol m^{-3} respectively (Fig. 3C). Nevertheless, this parameter seems less critical in the solubility range of typical materials such as PDMS and COC. In contrast, the solubility affected to some extent the reoxygenation rate as we observed after two hours a ΔpO_2 of 3.5 mmHg for an adhesive of S = 0.5 mol m^{-3} versus 17 mmHg for S = 3 mol m^{-3} (Fig. 3D, Table S3†).

Remarkably, these simulations allowed the effect of adhesive properties on on-chip oxygen control to be disentangled. Our results showed that despite the predominance of impermeable glass in our chip (more than 95% of the channel surface), the oxygen concentration in the channel is significantly affected by the adhesive properties. We demonstrated that, within the studied ranges, the oxygen diffusion coefficient is a determinant parameter of the oxygen control. For precise control, only adhesive materials with an oxygen diffusion rate lower than
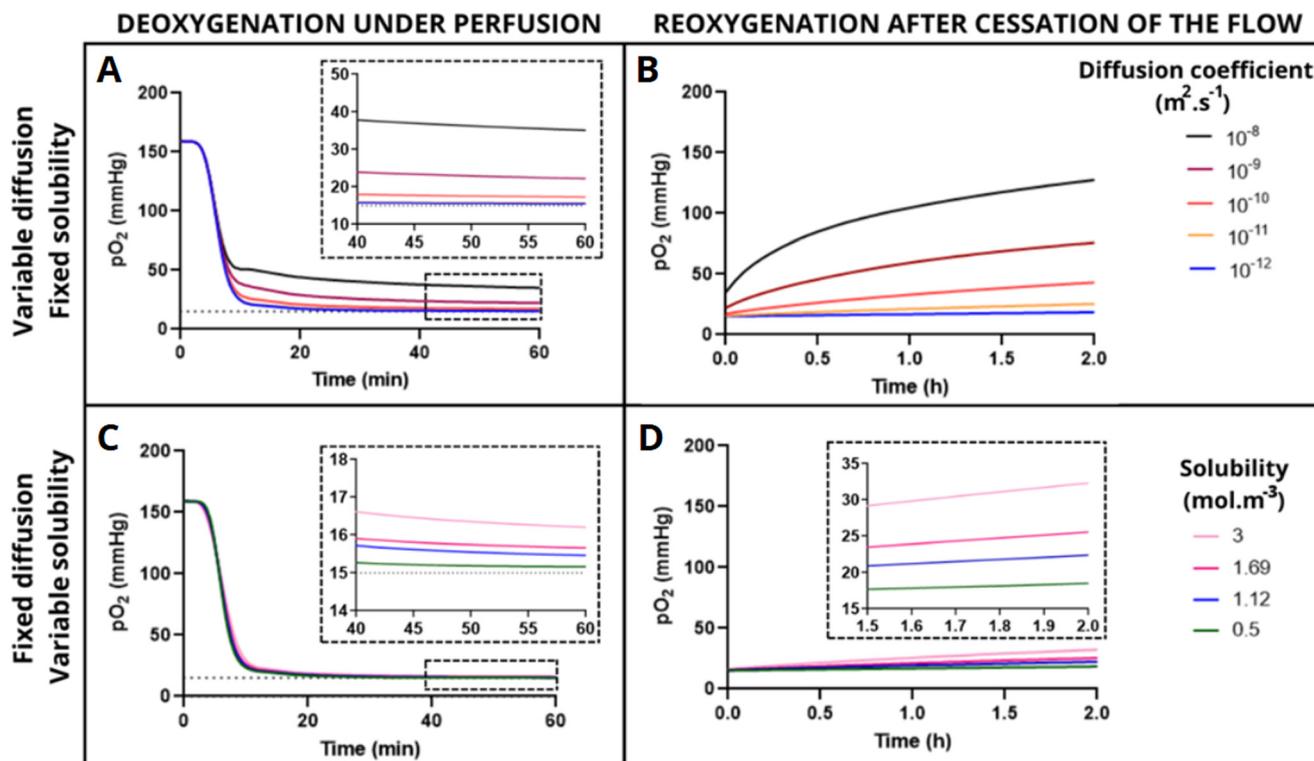
Fig. 3 Finite element simulation of pO_2 inside the chip for different adhesive properties. (A) Deoxygenation inside the chip under perfusion at 10 µL min^{-1} of pre-equilibrated water at pO_2 = 15 mmHg. Under these conditions, the chip is assembled with a 100 µm adhesive layer with a solubility of S = 1.12 mol m^{-3} and varying diffusion coefficients. (B) Reoxygenation inside the chip after cessation of the flow for a chip assembled with a 100 µm adhesive layer at a solubility of S = 1.12 mol m^{-3} and varying diffusion coefficients. (C) Deoxygenation inside the chip under perfusion at 10 µL min^{-1} of pre-equilibrated water at pO_2 = 15 mmHg. The chip is assembled with a 100 µm adhesive layer with a diffusion coefficient of D = 4.6 × 10^{-12} m^2 s^{-1} and varying solubility values. (D) Reoxygenation inside the chip after cessation of the flow for a chip assembled with a 100 µm adhesive layer at a diffusion coefficient of D = 4.6 × 10^{-12} m^2 s^{-1} and varying solubility values.

D = 10^{-12} m^2 s^{-1} should be used. All simulations in the rest of this study were then conducted using the physical properties of a low-permeability material (D = 4.6 × 10^{-12} m^2 s^{-1}, S = 1.12 mol m^{-3}).

Impact of the adhesive geometry on oxygen control of the hybrid glass chip

We next examined the impact of the adhesive layer geometry, specifically its thickness and width, on oxygen control in the hybrid glass chip. As all adhesive materials exhibit oxygen solubility, the key parameter of oxygen control may be the adhesive's volume as it could act as an oxygen reservoir.

Changing the adhesive width alters both the total adhesive volume and the distance between the ambient air and the fluidic channel (Fig. 4A). To perform simulations, we considered the adhesive width to be uniformly distributed along the channel. Different widths were tested, among which were experimentally practical ones (1 and 10 mm) and extreme conditions (0.1 mm). Interestingly, the adhesive width did not affect significantly the equilibration time, (around 25 min required) for all the tested adhesive widths (Fig. 4B, Table S4†). On the opposite, it has a significant impact on reoxygenation: after 2 h we measured a ΔpO_2 of 20.4 mmHg and 7.2 mmHg for

a width of 0.1 and 10 mm, respectively. Optimal performance was achieved with the 10 mm width as the distance between the ambient air and the central channel was higher, leading to a slower entry of oxygen into the channel (Fig. 4C). This suggests that the oxygen gradient established within the adhesive is a key factor of oxygen control (Fig. S5†). Inside the 0.1 mm adhesive (Fig. S6†), a steep gradient is observed, as the pO_2 gradient develops over a short distance within the adhesive layer. For the other two cases (1 mm and 10 mm), the distance over which the O$_2$ gradient is established is smaller than the total thickness of the adhesive layer. At a short timescale, the transport layer exhibits a characteristic width of $\sqrt{(Dt)}$. Once this limit is reached, the system stabilizes at a plateau corresponding to the maximum solubility of the adhesive. We conclude that a minimal width of 1 mm should thus be used to prevent significant reoxygenation. The following study was conducted using a width higher than 1 mm.

We next examined the impact of varying the adhesive thickness on oxygen control with thicknesses ranging from 20 µm to 300 µm (Fig. 5A). In contrast to the previous case, increasing the thickness does not affect the oxygen diffusion gradient but increases the volume of the adhesive, and consequently, the amount of oxygen stored inside the adhesive. Importantly, it also affects the surface area between
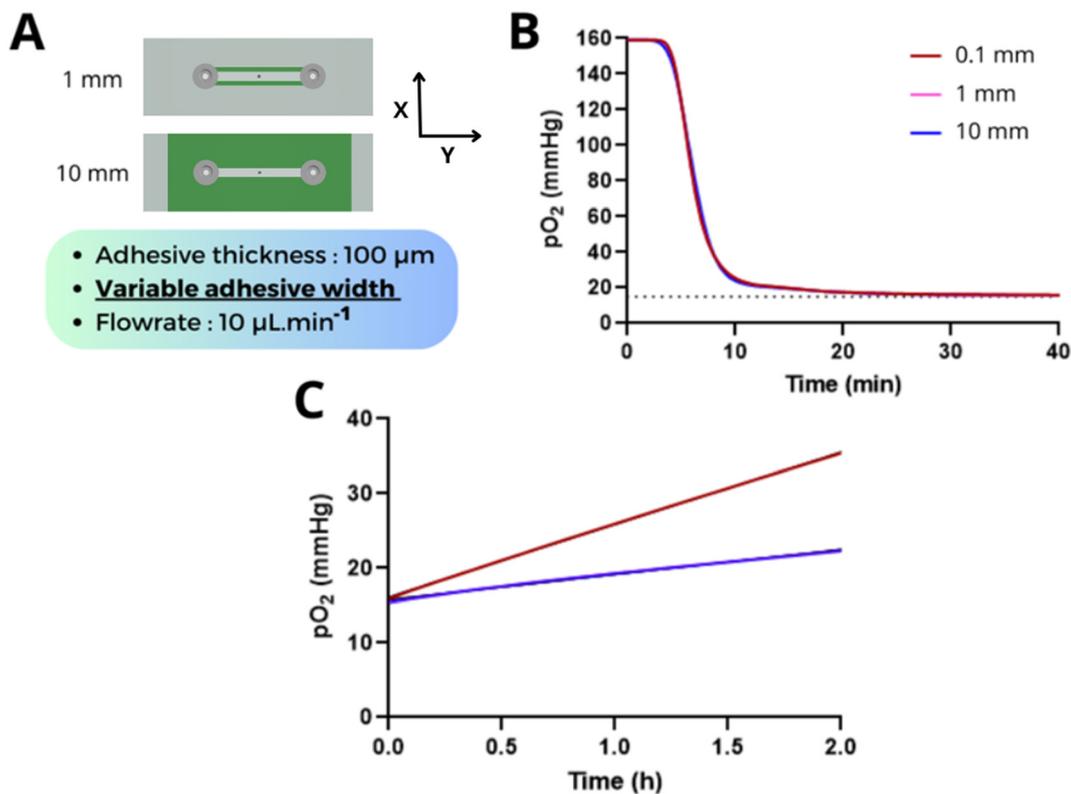
Fig. 4 Finite element analysis of varying adhesive widths for a thickness of 100 μm ($S = 1.12$ mol m^{-3} and $D = 4.6 \times 10^{-12}$ m^2 s^{-1}). (A) Schematic of two different widths of adhesive (1 mm and 10 mm) for assembling the glass slides (top view). The width of the adhesive is uniformly distributed along the channel. (B) Deoxygenation under perfusion with 15 mmHg pO$_2$ pre-equilibrated water at 10 μL min^{-1}. The width does not have a strong effect on the time to reach the target. (C) Reoxygenation during 2 h after cessation of the flow. A fast reoxygenation rate is observed for a short width (0.1 mm) while reoxygenation rates for 1 and 10 mm widths are very similar (overlaid curves) and slower.

the adhesive and the fluidic channel. We observed that increasing the adhesive thickness significantly decreases the deoxygenation slope from −17 to −37 mmHg min^{-1} for a thickness of 300 and 20 μm respectively (Fig. 5B, Table S5†). The equilibration time was 2.7 times higher for 300 μm adhesive compared to 20 μm (Fig. 5B). This is likely a consequence of the increased adhesive volume, which necessitates more time for the removal of oxygen inside the adhesive layer during perfusion. The reoxygenation was also strongly affected by the adhesive thickness (Fig. 5C): after 2 h, we measured a ΔpO$_2$ of +3.7 and +13 mmHg for thicknesses of 20 and 300 μm, respectively.

This finite element analysis demonstrates that the adhesive thickness is also a critical parameter and should be minimized to optimize the on-chip oxygen control. However, targeting a thickness of 20 μm would necessitate the utilization of cleanroom techniques (e.g. spin coater) which would not align with our initial goal of developing a low-tech, low-cost protocol. We evidenced that a hybrid glass chip assembled with a 100 μm layer is a good compromise for on-chip oxygen control performance. The pO$_2$ target of 15 mmHg was reached within 25 min and minimal reoxygenation, below 4 mmHg per 2 h, was observed after flow cessation.

Overall, this finite element provided a thorough examination of adhesive properties and their effects on

oxygen control in a glass hybrid chip. We identified critical parameters of adhesive: a diffusion coefficient below 10^{-12} m^2 s^{-1} along with the design geometry, such as a width higher than 1 mm and a thickness lower than 100 μm.

Identifying a suitable adhesive material for optimal oxygen control in the hybrid glass chip

The next step was to experimentally validate these criteria by fabricating hybrid glass–adhesive chips with different adhesive candidates. Silicon glue commonly used in microfluidics was quickly ruled out due to its noticeable impact on the oxygen level (Fig. S4†). Due to the unavailability of information regarding diffusion coefficients or oxygen solubility of commercially available adhesive, we selected adhesive materials based on their oxygen permeability data. It is worth noting that permeability is given by dynamic characterization: it measures the passage of oxygen through the material of interest in an oxygen pressure gradient, whereas our previous parameters, diffusion and solubility, were passive descriptors of the material. Epoxy adhesives have been reported to have a very low oxygen permeability of around 10^{-11} cm^3 (STP) cm cm^{-2} s^{-1} cmHg^{-1} (ref. 18) close to the one of COC (ranging from 10^{-11} to 10^{-10} cm^3 (STP) cm cm^{-2} s^{-1} cmHg^{-1} [19] at 25 °C). This is mainly due to the presence of polar groups within the epoxy (e.g.,
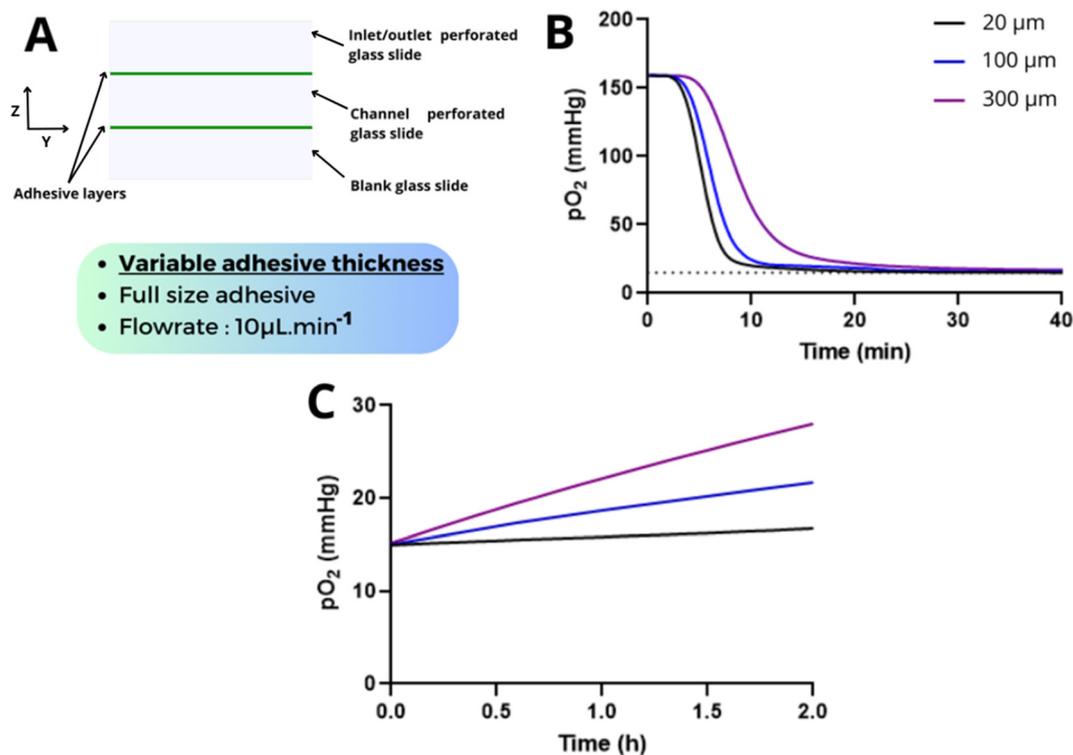
Fig. 5 Finite element analysis of varying adhesive thicknesses for an adhesive entirely covering the glass slides (S = 1.12 mol m^{-3} and D = 4.6 × 10^{-12} m^2 s^{-1}). (A) Schematic of varying thicknesses (20 μm, 100 μm, 300 μm) of the adhesive layer in the hybrid glass chip (cross section). (B) Deoxygenation under 10 μL min^{-1} perfusion with 15 mmHg pO$_2$ pre-equilibrated water. Increasing the adhesive thickness increases the time needed to reach the target. (C) Reoxygenation during 2 h after cessation of the flow. Increasing the adhesive thickness increases the slope of the reoxygenation.

hydroxyl, amino, *etc.*) which induce hydrogen bonding between polymeric chains and restrain motion in the polymeric network. Bonding and segment mobilities are central to the solubility and diffusivity of penetrants, such as oxygen, within the polymeric structure.[20] We also identified dental resins as potential adhesives for our application as they are made of a mixture of methacrylate and SiO$_2$ nanoparticles,[21] which are known to reduce oxygen diffusion and solubility.[16] One advantage of dental resins is their UV-sensitivity, allowing for rapid polymerization and biocompatibility.

To assess experimentally the potential of these adhesive materials on the oxygen control of this hybrid glass chip, a liquid with an oxygen level controlled using an Oxalis system[9] was flowed through the chip, and the oxygen level was continuously measured within the chip using a Pyroscience oxygen sensor. We perfused glass–epoxy (Fig. 6A) and glass–dental resin chips with the Oxalis set at different flow rates (10, 40 and 100 μL min^{-1}) with water pre-equilibrated at 15 mmHg to explore the potential of these hybrid glass chips. The experimental results were then compared with a simulation of a glass–adhesive chip for the low permeability adhesive tested so far (D = 4.6 × 10^{-12} m^2 s^{-1}, S = 1.12 mol m^{-3}).

As shown in Fig. 6B, the glass–epoxy chip allowed the target pO$_2$ to be reached slightly faster than the glass–dental resin chip for all the flow rates tested. With a glass–epoxy chip, a 15 mmHg pO$_2$ was reached in 1.5 min for 100 μL min^{-1} and 23.5

min for 10 μL min^{-1} *versus* 5 min for 100 μL min^{-1} and 42.5 min for 10 μL min^{-1} using the dental resin, respectively. The glass–epoxy chip showed a similar variation in pO$_2$ compared to the simulation, indicating that the epoxy material likely exhibits oxygen diffusion and solubility properties comparable to those of the simulated adhesive. The hybrid glass–dental resin chip was discarded at this stage as it did not allow the oxygen target level to be reached in a reasonable time.

To evaluate the reoxygenation within the glass hybrid chip, we conducted pO$_2$ measurements during 2 h under static conditions after 1 h of perfusion with a pre-equilibrated liquid. We measured an increase of only 0.6 mmHg per 2 h in the glass–epoxy chip (Fig. 6C) demonstrating limited reoxygenation, comparable to the glass–adhesive chip simulation. This highlights the potential of epoxy adhesive to be used for the hybrid–glass chip fabrication. This easy-to-fabricate microfluidic chip, assembled with a low-cost adhesive and subsequently perfused with the Oxalis, proves to be a powerful tool for oxygen control with a fast response time.

Cell culture inside the glass–epoxy chip and measurement of cellular respiration

Measurement of cellular respiration is among the most fundamental techniques for understanding cellular
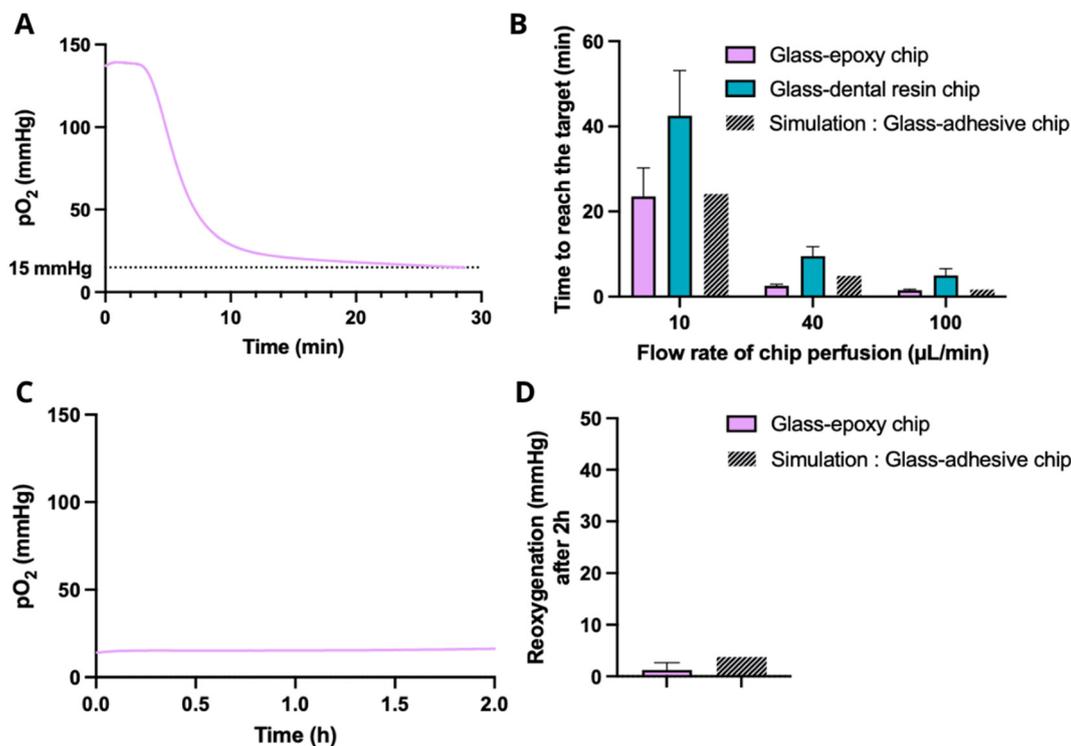
Fig. 6 Experimental data using chips fabricated with two different types of adhesive layers: epoxy or dental resin (width: 11.5 mm in the x direction and 18.5 mm in the y direction, thickness: 100 ± 20 μm). (A) Deoxygenation measured in a glass–epoxy chip during the perfusion at 10 μL min^{-1} of water pre-equilibrated at pO_2 = 15 mmHg. (B) Time to reach the pO_2 target in the glass–epoxy and glass-dental resin microfluidic chips during the perfusion of water pre-equilibrated at pO_2 = 15 mmHg. Three different flow rates were tested: 10 μL min^{-1}, 40 μL min^{-1}, and 100 μL min^{-1} (N = 3 experiments for each flow rate) and compared to the glass–adhesive chip simulation (conditions as in Fig. 5). (C) Reoxygenation measured inside the glass–epoxy chip during 2 h after cessation of the flow. (D) Reoxygenation after 2 h (N = 3 experiments) compared to the glass–adhesive chip simulation (conditions as in Fig. 5).

bioenergetics.[22] Since the reoxygenation inside our hybrid glass–epoxy chip is negligible (ΔpO_2 = 0.6 mmHg per 2 h), this method seems promising for quantifying oxygen consumption by cells. It's worth mentioning that conventional measurements in cell culture plastic plates are susceptible to constant diffusion of O_2 from ambient air through the plastic[23] and require a correction algorithm that aims at discriminating the biological oxygen consumption rate from the flux of oxygen stemming from the cell environment. Our hybrid glass chip does not require any correction as it could provide direct measurement of cell oxygen consumption and could thus be used as a cell respirometer.

Common methods to measure cellular oxygen consumption are performed at an ambient air oxygen level (20.9%), which inherently represents hyperoxic conditions compared to *in vivo* settings.[2] A more precise respirometer would need to recapitulate physiological or pathological oxygen levels to properly evaluate cell oxygen consumption (*i.e.* 5.6% in peri-bronchial lung tissues, 8.5% in the breast, 3.4% in the brain[2]). Therefore, combining precise oxygen control provided by the Oxalis system[9] with this hybrid glass–epoxy chip could open up new biological questions, such as how cells adjust their oxygen consumption in response to the surrounding concentration.

We first demonstrated that the glass hybrid chip is compatible with cell culture. A549 lung cancer cells were cultured for 12 h in the glass–epoxy chip (Fig. 7A) under static conditions. The high cell viability of 98.8% (Fig. 7B) confirmed the epoxy adhesive layer cytocompatibility. Next, to evaluate the potential of our approach as a cell respirometer, we conducted a first proof of concept by perfusing the chip with the Oxalis at different oxygen levels and measuring cell respiration after stopping the flow. Oxygen measurements in the chip were conducted using oxygen spots incorporated directly at the bottom of the chip, close to the cells, allowing for the assessment of cell respiration under static conditions. In Fig. 7C, we demonstrated the Oxalis system's capability to rapidly set the glass–epoxy chip to a target oxygen value across a wide range of pO_2 (from 50 to 150 mmHg). We measured an O_2 consumption rate of 0.8 mmHg min^{-1} for a monolayer of A549 lung cancer cells being exposed to a pO_2 of 50 mmHg and a rate of 1.4 mmHg min^{-1} after being exposed to a pO_2 of 80 mmHg. These results suggest that at a low oxygen level, the A549 cells modulate their metabolism in response to the oxygen level. This not only highlights the system's ability to maintain precise oxygen conditions but also enables the measurement of cellular respiration at a specific and controllable pO_2, rather than being limited to ambient pO_2 as is the case with conventional respirometers.
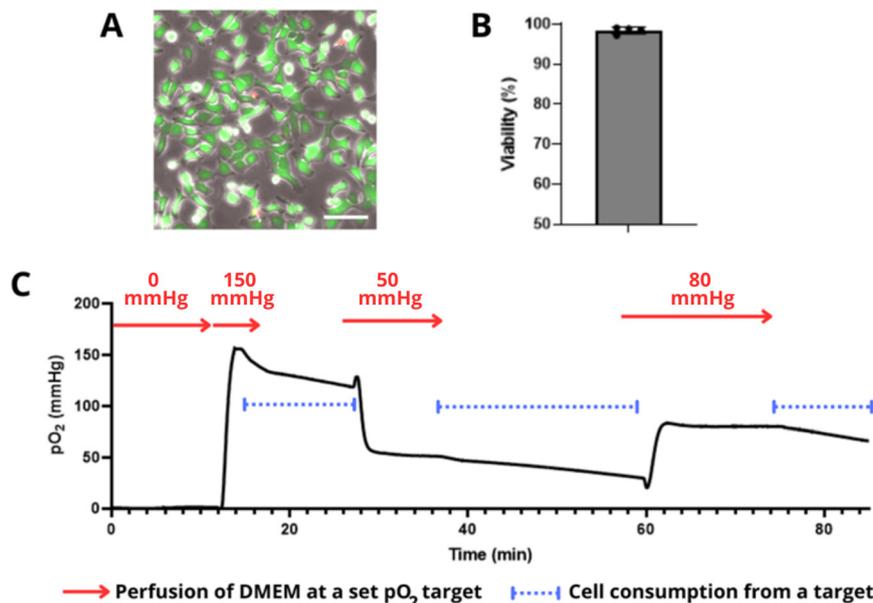
Fig. 7 (A) Image of live dead assays of the A549 monolayer after 12 h in the glass–epoxy chip (scale bar: 100 μm). (B) Cell viability after 12 h in the glass–epoxy chip. (C) Cellular oxygen consumption over time inside the glass–epoxy chip. The chip is perfused at 10 μL min⁻¹ with pre-equilibrated DMEM at various $p\text{O}_2$ values, and then the flow is stopped to measure cellular oxygen consumption under static conditions.

This proof of concept sets the stage for future biological studies employing this hybrid glass chip combined with oxygen control as a cell respirometer under physiological or pathological oxygen conditions. It also raises the possibility of pre-conditioning cells to specific oxygen levels for a defined period and determining whether varying the hypoxic culture duration subsequently affects oxygen consumption when returned to physioxia. To conclude, this system enables the measurement of both adaptability and oxygen consumption under highly precise conditions, a capability not previously achievable with conventional respirometers.

Discussion

Finely regulating oxygen levels in microfluidic devices is critical for cell-based applications. On-chip oxygen control strategies are mainly based either on gas channels[5] or perfusion of a pre-equilibrated liquid at a set target.[9] Regardless of the oxygen control method or of the application, the choice of low oxygen permeability materials is paramount; glass chips are well-suited due to their oxygen tightness, but their fabrication processes are complex and clean-room facilities are often required.[11] A major challenge lies in the development of a low-tech microfluidic chip fabrication method that exhibits oxygen permeability properties comparable to glass.

We explored the possibility of fabricating low-tech hybrid glass chips having gas permeability properties equivalent to those of a full glass chip. Hybrid glass–adhesive chips were produced by assembling glass components with two layers of adhesives. We proposed a two-step protocol to define the crucial parameters for selecting and designing the adhesive layers: i)

the time required to reach an oxygen level when perfusing the chip with pre-equilibrated water and ii) the on-chip reoxygenation after perfusion stops. Using this two-step protocol, we produced both finite element simulations and experimental data. Finite element analysis allowed us to decipher the contribution of various intrinsic parameters of the adhesive materials such as the oxygen diffusion coefficient and oxygen solubility. It also evidences the impact of parameters related to the chip fabrication such as the adhesive's layer width and thickness. Interestingly, our study unveiled a noteworthy influence of the adhesive layers on the oxygen control capabilities, although the adhesive corresponds only to 5% of the surface of the channel. We concluded that an adhesive material with an oxygen diffusion rate lower than 10^{-12} m² s⁻¹ and with a solubility lower than 1.1 mol m⁻³ should be preferred. As oxygen solubility is inherent in all adhesives, they will always act as oxygen reserves. Our simulations indicated that the adhesive thickness should be minimized but can be maintained at around 100 μm to achieve good performance.

Adhesives filling these criteria and allowing an assembly outside of clean room environments were next chosen. Among the low gas permeability materials, we specifically selected highly viscous adhesives, namely epoxy and dental resin, to enable easy manual application of an approximately 100 μm layer. We experimentally confirmed the compatibility of these adhesives with on-chip oxygen control. The glass–epoxy chip allowed fine and rapid oxygen-control: the $p\text{O}_2$ target was reached in 1.5 min for 100 μL min⁻¹, and 23.5 min for 10 μL min⁻¹. The glass–epoxy chip demonstrates a $p\text{O}_2$ variation similar to that of simulations, indicating that the epoxy material likely exhibits oxygen diffusion and solubility properties comparable to those of the simulated adhesive (D

$= 4.6 \times 10^{-12}$ m^2 s^{-1}, $S = 1.12$ mol m^{-3}). These findings suggest that our approach could be used as an empirical method to characterize adhesive properties, such as the diffusion coefficient and solubility.

The excellent oxygen control performance of the glass–epoxy chip suggests that similar performance could be achieved with more complex designs fabricated with SU8, which is a common epoxy-based resin used for photolithography. This oxygen control could certainly be further improved by incorporating glass nanoparticles into the adhesive material which would decrease both the oxygen solubility and oxygen diffusion rate by creating longer and more tortuous pathways for oxygen.[16]

Furthermore, this glass–epoxy chip serves as a tight system, effectively preventing reoxygenation (only 0.6 mmHg in 2 hours) under static conditions. This renders the hybrid glass chip compatible with cell respiration measurement under constant or transient physiological or pathological oxygen conditions. These interesting features were experimentally demonstrated with lung cancer cell lines. The hybrid system is highly versatile in terms of oxygen conditions before or during cell respiration measurement unlike the gold standard methods such as the multi-well plate-based assay[22] measuring cell consumption only from ambient air conditions. In addition, we also demonstrated the ability of our device to be used in a completely different context: plasma-based chemical reactions (Fig. S7†). These additional experiments demonstrated the potential of this hybrid glass chip for on-chip applications beyond cell-based ones.[24]

Conclusion and perspectives

In this study, we characterized the oxygen properties of a hybrid glass–adhesive chip by employing a two-step protocol, monitoring deoxygenation under flow and reoxygenation under static conditions. We demonstrated the crucial role of adhesive properties—particularly oxygen diffusion and solubility—in achieving gas-tight microfluidic systems for precise oxygen control. By directly comparing finite element analysis with experimental data, we identified epoxy as the highest-performing adhesive for fabricating a hybrid chip compatible with the perfusion of pre-equilibrated solutions at precise oxygen levels. Our hybrid glass–epoxy chip provides a versatile platform for applications such as cell respiration assays, as well as broader uses beyond cell biology, including plasma-based chemical reactions and other microfluidic processes. Combining the precise characterization of the chip with the very fast response time of an Oxalis system to reach a pO_2 target[9] could have various applications both in life sciences (sleep apnea,[25] ischemia–reperfusion,[26] cancer) and in chemistry (carboxylation of p-nitrophenyllithium,[27] flow synthesis of non-symmetrical urea utilizing CO_2 as a key building block[8] or other fast liquid reactions). Beyond oxygen-sensitive reactions, this system has the potential to precisely control other gases within flow microreactors[28,29] such as carbon monoxide, hydrogen or CO_2.

Experimental section

Chip fabrication

We used optical glass slides in soda lime (70% silicon dioxide, 15% sodium oxide, 9% calcium oxide). A drill (DREMEL model 4000) at 6000 RPM was first used to create the central channel on conventional microscopy glass slides (76 × 26 × 1 mm, CARL ROTH, 0656). Diamond tips of 3 mm in diameter were used to create two holes for inserting a diamond disk to create the rectangular chamber of 3 mm × 37 mm. This channel width of 3 mm has been chosen to allow for manual insertion of the oxygen sensor spot into the channel and to ensure that at a flow rate of 10 µL min^{-1}, negligible shear stress is applied for the cell culture experiment. Another reason for this choice is that the large volume of the channel allows the flow to be stopped briefly in the presence of cells without rapidly depleting the oxygen. Diamond tips of 2 mm were then used to create the two holes for the top glass slide. Alternatively, a laser ablation machine (GCC C180II 12–40 W CO$_2$) can be used with the following parameters: speed 30, power 100, PPI 400, repeat 20 times. The glass slides were immersed in water during drilling or ablation to prevent them from breaking.

The three glass slides were assembled with two layers of adhesive. The glue was spread manually with a pipette tip and the glass slides were pinched to spread the glue as uniformly as possible. The glue (Epoxy Loctite 9492 and dental resin Filtek Supreme XTE) was allowed to dry for 2 h at room temperature before gluing the third slide. Fluidic inlets (Nanoports, IDEX N-333) were attached with epoxy (Araldite 2000). The adhesive width was 11.5 mm in the x direction ((glass slide width 26 mm – channel width 3 mm)/ 2), and 18.5 mm in the y direction ((glass slide length 76 mm – channel length 37 mm)/2) (Fig. 1A). Using a micrometer, the thickness of each glass slide and the thickness of the total chip were measured in order to ensure that the thickness of the adhesive layers was approximately 100 µm. An experimental error range of ±20 µm was accepted.

Before starting the experiments, the chip was kept overnight in a 70 °C oven to ensure that all the solvents are evaporated from the glue. After the experiment, the chip can be recycled by placing it in a chloroform bath at 40 °C for 1 hour to recycle the fluidic connectors and then in an oven at 500 °C for 24 hours to remove the adhesive layer and recycle the glass slides.

Fluidic line

Our oxygen controller Oxalis was used to perfuse the microfluidic chip as described in the study of Bouquerel et al.[9] A fused silica capillary (Postnova, Z-FSS-250350) with sleeves 1/16e and 1/32e (F-242, F-376) was used to connect the Oxalis to the custom glass chip. A 2-step method was used to accelerate the deoxygenation time within the reservoir by carrying out first a N$_2$ blowing step allowing fast oxygen removal[9] inside the inlet reservoir: targeting first 0 mmHg then 15 mmHg leading faster to 15 mmHg in the

liquid. This strategy is based on Fick's law, which states that the oxygen diffusion rate increases with the oxygen concentration gradient.

On-chip oxygen measurement

An oxygen optical sensing spot (2 mm^2 cut from an OXSP5-ADH Pyroscience) was glued on the bottom glass slide of the chip before chip bonding. We set the channel width at 3 mm to allow for manual insertion of the oxygen sensor spot into the channel. This sensor is specified for an optimum measuring range of 0 to 400 mmHg oxygen. This manufacturing process enables the on chip oxygen level to be precisely measured. On-chip oxygen measurement was performed with a Pyroscience board (PICO$_2$). According to the supplier specifications, the accuracy of pO_2 measurement ranges from 0.15 to 1.5 mmHg for pO_2 levels between 7.5 and 150 mmHg.

COMSOL simulation

COMSOL Multiphysics v6.0 was used to simulate the hybrid glass chip in 3D (Fig. S2†). The varying concentrations of dissolved oxygen through the system were modeled using relevant mass transfer equations, which take into account both advection (based on fluid flow at a specified velocity along the channel) and diffusion (based on Fick's law).

In the adhesive layer, we used the diffusion law to describe the oxygen profile: $\frac{d[O_2]}{dt} = D\nabla^2[O_2]$. In the liquid, the oxygen profile is described by the diffusion–advection equation: $\frac{d[O_2]}{dt} = D\nabla^2[O_2] + v\nabla[O_2]$ with v (m s^{-1}) being the velocity field: a Poiseuille flow of average value $v = \frac{Q}{S}$ where Q is the flow rate (m^3 s^{-1}) and S (m^2) is the channel cross-section. The boundary conditions at polymer/air and polymer/water interfaces are described by a partition coefficient: $[O_2]_m = K_{m/air}[O_2]_{air}$ and $[O_2]_m = K_{m/water}[O_2]_{water}$. The boundary conditions at the glass/liquid interface are set as no mass transfer conditions.

These coefficients are calculated using the values of $[O_2]_m$, $[O_2]_{air}$ and $[O_2]_{water}$ at equilibrium under atmospheric conditions. All the parameters used for the simulations are given in Table S1.† The results were given by COMSOL in mol m^{-3} and converted in mmHg to plot the figures using a conversion based on Henry's law: $pO_2 = [O_2] \times 159/0.279$, with 159 mmHg being the pO_2 in ambient air (20.94% of 760 mmHg), and 0.279 mol m^{-3} being the concentration of water at equilibrium with ambient air. The concentration of oxygen in the pre-equilibrated water is 0.0262 mol m^{-3} (corresponding to 15 mmHg).

Cell culture

Human lung cancer cells A549 were purchased from ATCC (#CCL-185). The cells were routinely tested for mycoplasma contamination using a qPCR-based method (VenorGem Classic, BioValley, #11-1250) and authenticated by short

tandem repeat (STR) profiling (GenePrint 10 system, Promega, #B9510). The cells were maintained in DMEM 1×-Glutamax (Gibco) supplemented with 10% fetal bovine serum (Biosera) and 1% penicillin streptomycin antibiotic solution (Gibco) at 37 °C in a humidified atmosphere of 5% CO$_2$. The cells were seeded in glass–epoxy microfluidic chips at a density of 0.5 million cells per mL after fibronectin coating for 30 min at 37 °C (Gibco 33010018, 10 μg mL^{-1}). The large volume of the channel (approximately 100 μL) allows the flow to be stopped briefly in the presence of cells without rapidly depleting the oxygen, allowing cell adhesion under 18.6% O$_2$ at the beginning of the experiment.

Plasma chemical reaction on-chip

The gases (Ar or O$_2$ with a purity of 99.99%) were introduced into the chip using mass flow controllers (Bronkhorst MFC EL-FLOW prestige) at 3 ml min^{-1}. Before reaching the chip, the gas stream was bubbled in a vial containing pure piperidine (liquid) maintained at 30 °C. This was used as a bubbler to enrich the carrier gas stream with the substrate (piperidine) which subsequently will be treated under plasma conditions. For this purpose, the chip was equipped with a planar copper electrode (adhesive copper tape RS Pro ref: 176-7498) that allowed the delivery of the electrical current. A sinusoidal signal permitted the initiation of the plasma, it was delivered by an alternative function generator (AFG – sinusoidal wave at 2 kHz) and amplified with a high voltage amplifier (Trek 20/20c) along with a crocodile type clamp to connect to the chip's electrode. The products formed in the gas phase were trapped using a round bottom flask filled with ethyl acetate at 0 °C, and the liquid phase containing trapped products was analyzed by GC/MS (gas chromatography coupled to mass spectrometry). The piperidine was treated with Ar plasma as well as O$_2$ plasma (positive control).

Data availability

The data supporting this article have been partially included as part of the ESI† and the others are available upon request from the authors.

Conflicts of interest

This work was supported by Fluigent and Institut Curie.

Acknowledgements

research by offering oxygen sensors. We thank Guillem Wetherel Matheu, a master student of the team, for proceeding some of the experiments included in Fig. 6, allowing to confirm that similar results were obtained from different users. We thank Maxime Simon and Alex Barbier-Chebbah for careful proofreading of the manuscript.

Notes and references

1 E. Ortiz-Prado, J. F. Dunn, J. Vasconez, D. Castillo and G. Viscor, Partial pressure of oxygen in the human body: a general review, *Am. J. Blood Res.*, 2019, **9**(1), 1–14.

2 T. P. Keeley and G. E. Mann, Defining Physiological Normoxia for Improved Translation of Cell Physiology to Animal Models and Humans, *Physiol. Rev.*, 2019, **99**, 161–234, DOI: **10.1152/physrev.00041.2017**.

3 C. A. Hone and C. O. Kappe, Membrane Microreactors for the On-Demand Generation, Separation, and Reaction of Gases, *Chem. – Eur. J.*, 2020, **26**(58), 13108–13117, DOI: **10.1002/chem.202001942**.

4 T. P. Petersen, A. Polyzos, M. O'Brien, T. Ulven, I. R. Baxendale and S. V. Ley, The oxygen-mediated synthesis of 1,3-butadiynes in continuous flow: Using teflon AF-2400 to effect gas/liquid contact, *ChemSusChem*, 2012, **5**(2), 274–277, DOI: **10.1002/cssc.201100339**.

5 R. Koens, Y. Tabata and J. C. Serrano, et al., Microfluidic platform for three-dimensional cell culture under spatiotemporal heterogeneity of oxygen tension, *APL Bioeng.*, 2020, **4**(1), 016106, DOI: **10.1063/1.5127069**.

6 C. J. Mallia and I. R. Baxendale, The Use of Gases in Flow Synthesis, *Org. Process Res. Dev.*, 2016, **20**(2), 327–360, DOI: **10.1021/acs.oprd.5b00222**.

7 Y. Gao, G. Stybayeva and A. Revzin, Fabrication of composite microfluidic devices for local control of oxygen tension in cell cultures, *Lab Chip*, 2019, **19**(2), 306–315, DOI: **10.1039/C8LC00825F**.

8 D. H. Khan, S. A. Roberts, J. R. Cressman and N. Agrawal, Rapid Generation and Detection of Biomimetic Oxygen Concentration Gradients in Vitro, *Sci. Rep.*, 2017, **7**(1), 1–11, DOI: **10.1038/s41598-017-13886-z**.

9 C. Bouquerel, W. César and L. Barthod, et al., Precise and fast control of the dissolved oxygen level for tumor-on-chip, *Lab Chip*, 2022, **22**(22), 4443–4455, DOI: **10.1039/d2lc00696k**.

10 D. Wu and P. Yotnda, Induction and testing of hypoxia in cell culture, *J. Visualized Exp.*, 2011, **54**, 4–7, DOI: **10.3791/2899**.

11 M. Castaño-Álvarez, D. F. Pozo Ayuso, M. García Granda, M. T. Fernández-Abedul, J. Rodríguez García and A. Costa-García, Critical points in the fabrication of microfluidic devices on glass substrates, *Sens. Actuators, B*, 2008, **130**(1), 436–448, DOI: **10.1016/j.snb.2007.09.043**.

12 C. Wang, H. Fang and S. Zhou, et al., Recycled low-temperature direct bonding of Si/glass and glass/glass chips for detachable micro/nanofluidic devices, *J. Mater. Sci. Technol.*, 2020, **46**, 156–167, DOI: **10.1016/j.jmst.2019.11.034**.

13 S. I. Funano, N. Ota and Y. Tanaka, A simple and reversible glass-glass bonding method to construct a microfluidic device and its application for cell recovery, *Lab Chip*, 2021, **21**(11), 2244–2254, DOI: **10.1039/d1lc00058f**.

14 H. Y. Wang, R. S. Foote, S. C. Jacobson, J. H. Schneibel and J. M. Ramsey, Low Temperature Bonding for Microfabrication of Chemical Analysis Devices, *Sens. Actuators, B*, 1997, **45**(3), 199–207, DOI: **10.1016/S0925-4005(97)00294-3**.

15 S. R. McKeown, Defining normoxia, physoxia and hypoxia in tumours - Implications for treatment response, *Br. J. Radiol.*, 2018, **87**(1035), 1–12, DOI: **10.1259/bjr.20130676**.

16 M. Zabihzadeh Khajavi, A. Ebrahimi and M. Yousefi, et al., Strategies for Producing Improved Oxygen Barrier Materials Appropriate for the Food Packaging Sector, *Food Eng. Rev.*, 2020, **12**(3), 346–363, DOI: **10.1007/s12393-020-09235-y**.

17 M. Zahorodny-Burke, B. Nearingburg and A. L. Elias, Finite element analysis of oxygen transport in microfluidic cell culture devices with varying channel architectures, perfusion rates, and materials, *Chem. Eng. Sci.*, 2011, **66**(23), 6244–6253, DOI: **10.1016/j.ces.2011.09.007**.

18 Q. Zhang, Y. C. Wang and C. G. Bailey, et al., Quantification of gas permeability of epoxy resin composites with graphene nanoplatelets, *Compos. Sci. Technol.*, 2019, **184**, DOI: **10.1016/j.compscitech.2019.107875**.

19 M. C. Celina and A. Quintana, Oxygen diffusivity and permeation through polymers at elevated temperature, *Polymer*, 2018, **150**, 326–342, DOI: **10.1016/j.polymer.2018.06.047**.

20 H. Zargar, P. Zarei, D. Wong, C. Lam and E. Asselin, Transport of water and oxygen in epoxy-based coatings, *ChemRxiv*, 2022, preprint, DOI: **10.26434/chemrxiv-2022-b276b-v3**.

21 K. Cho, G. Rajan, P. Farrar, L. Prentice and B. G. Prusty, Dental resin composites: A review on materials to product realizations, *Composites, Part B*, 2022, **230**, DOI: **10.1016/j.compositesb.2021.109495**.

22 D. A. Ferrick, A. Neilson and C. Beeson, Advances in measuring cellular bioenergetics using extracellular flux, *Drug Discovery Today*, 2008, **13**(5–6), 268–274, DOI: **10.1016/j.drudis.2007.12.008**.

23 A. A. Gerencser, A. Neilson and S. W. Choi, et al., Quantitative microplate-based respirometry with correction for oxygen diffusion, *Anal. Chem.*, 2009, **81**(16), 6868–6878, DOI: **10.1021/ac900881z**.

24 J. Wengler, S. Ognier and M. Zhang, et al., Microfluidic chips for plasma flow chemistry: Application to controlled oxidative processes, *React. Chem. Eng.*, 2018, **3**(6), 930–941, DOI: **10.1039/c8re00122g**.

25 M. Minoves, J. Morand and F. Perriot, et al., An innovative intermittent hypoxia model for cell cultures allowing fast PO$_2$ oscillations with minimal gas consumption Briançon-Marjollet A. An innovative intermittent hypoxia model for cell cultures allowing fast PO$_2$ oscillations with minimal gas consumption, *Am. J. Physiol.*, 2017, **313**, 460–468, DOI: **10.1152/ajpcell.00098.2017**.

26 T. Chen and G. Vunjak-Novakovic, In Vitro Models of Ischemia-Reperfusion Injury, *Regener. Eng. Transl. Med.*, 2018, **4**(3), 142–153, DOI: **10.1007/s40883-018-0056-0.**

27 A. Nagaki, Y. Takahashi and J. I. Yoshida, Extremely fast gas/liquid reactions in flow microreactors: Carboxylation of short-lived organolithiums, *Chem. – Eur. J.*, 2014, **20**(26), 7931–7934, DOI: **10.1002/chem.201402520.**

28 A. Labiche, M. Norlöff, S. Feuillastre, F. Taran and D. Audisio, Continuous Flow Synthesis of Non-Symmetrical Ureas from CO_2, *Asian J. Org. Chem.*, 2023, **12**(3), DOI: **10.1002/ajoc.202200640.**

29 C. J. Mallia and I. R. Baxendale, The Use of Gases in Flow Synthesis, *Org. Process Res. Dev.*, 2016, **20**(2), 327–360, DOI: **10.1021/acs.oprd.5b00222.**